Atmos. Meas. Tech. Discuss., 7, 3549–3589, 2014
www.atmos-meas-tech-discuss.net/7/3549/2014/
doi:10.5194/amtd-7-3549-2014

Atmospheric
Measurement
Techniques
Discussions
Open Access

Refractory black carbon mass concentrations in snow and ice: method evaluation and inter-comparison with elemental carbon measurement

S. Lim[1,2], X. Faïn[1,2], M. Zanatta[1,2,3], J. Cozic[1,2], J.-L. Jaffrezo[1,2], P. Ginot[1,2,4], and P. Laj[1,2]

[1]Univ. Grenoble Alpes, LGGE, 38000 Grenoble, France
[2]CNRS, LGGE, 38000 Grenoble, France
[3]Laboratory of Atmospheric Chemistry, Paul Scherrer Institute, 5232 Villigen PSI, Switzerland
[4]IRD, OSUG, 38000 Grenoble, France

Received: 23 January 2014 – Accepted: 17 March 2014 – Published: 7 April 2014

Correspondence to: S. Lim (slim@lgge.obs.ujf-grenoble.fr)

Published by Copernicus Publications on behalf of the European Geosciences Union.

Abstract

Accurate measurement of black carbon (BC) mass concentrations in snow and ice is crucial for the assessment of climatic impacts. However, it is difficult to compare methods used to assess BC levels in the literature as they are not the same. The single particle soot photometer (SP2) method appears to be one of the most suitable to measure low concentrations of BC in snow and ice. However, deriving BC concentrations with SP2 is not straightforward and different measurement options may lead to different results. In this paper, we propose an optimized method for the quantification of refractory BC (rBC) in snow and ice samples using SP2. The paper reviews all the steps of rBC determination including SP2 calibration, correction for rBC particle aerosolization, and treatment of the samples. In addition, we compare the SP2 method and the thermal-optical method (Sunset organic carbon (OC)-elemental carbon (EC) aerosol analyzer with EUSAAR-2 protocol), using snow and firn samples with different characteristics from the Greenland Summit, the French Alps, the Caucasus, and the Himalayas. The EC : rBC ratio was 1.8 ± 1.2 for the Greenland site, 0.4 ± 0.2 for the Alpine site, 0.9 ± 0.3 for the Caucasus site, and 3.0 ± 1.2 for the Himalayan site. Careful investigation was undertaken of analytical uncertainties in both methods, concerning the analytical range of detection of BC, aerosolization correction for rBC, filtration efficiency of quartz fiber filter before EC analysis, the impact of dust, and pyrolyzed organic carbon artifacts during EC analysis. We conclude that the complexity of artifacts can lead to inaccurate rBC or EC determination. In particular, we observed significant under-estimation of EC due to incomplete filtration together with positive artifacts caused by OC. These results underline the need for careful assessment of the analytical technique and procedure for correct data interpretation.

1 Introduction

Black carbon (BC) only enters the atmosphere as a primary emission and mainly originates from incomplete combustion of biomass and fossil fuels. BC is the subject of increasing attention as it is the second most important component of global warming after CO_2 (Bond et al., 2013; Ramanathan and Xu, 2010). BC particles are ubiquitous in the atmosphere and, due to their relatively long residence time, can be efficiently transported over long distances once emitted above the boundary layer, as for example to high-altitude or high latitude sites in the Northern Hemisphere, where they are deposited with snow precipitation and on the surface of the snow. The deposited BC darkens the surface of the snow and ice and can modify the local radiative balance with potentially larger scale consequences for climate (Doherty et al., 2010; Flanner et al., 2007; Painter et al., 2013). The absolute rate of snow albedo reduction by BC and other absorbing particles is not particularly high, but it is of concern because even slight changes in solar absorption can accelerate snowmelt (Clarke and Noone, 1985; Hansen and Nazarenko, 2004; Warren, 1984). Hence, BC deposited on snow surfaces has been identified as a significant contributing factor that may increase snowmelt over the Himalaya and the Tibetan Plateau (Flanner et al., 2007; Ginot et al., 2013; Xu et al., 2009), although the exact impact has not yet been precisely quantified. The BC deposited in snow is also an important indicator in ice core studies (e.g., McConnell et al., 2007) as it provides information on the variability of combustion processes due to both natural and anthropogenic activities. Since multi-year observations of atmospheric BC concentrations are rare, long-term BC trends derived from ice cores studies are extremely useful to identify possible changes in its sources of emission.

The term “black carbon (BC)” is often used without a clear definition of its meaning (Petzold et al., 2013). It is now generally agreed that, when determined by thermal methods using its chemical properties, BC should be called “elemental carbon (EC)”, and “BC” should only be used for measurements obtained by optical methods using its light-absorbing properties. Thermal methods have been widely used to quantify EC mass concentrations in snow and ice in the Arctic (Aamaas et al., 2011; Hagler et al., 2007), the European Alps (Legrand et al., 2007; Thevenon et al., 2009), and the Himalayas (Ming et al., 2008, 2009) as well as in the atmosphere, and the EC values obtained using these methods have been termed "BC" in many studies. Optical methods are also widely used but usually for monitoring ambient BC. BC measured using optical methods should thus be called "equivalent BC (eBC)" since its mass concentration is indirectly determined by applying a mass absorption cross-section (MAC) of BC (Petzold et al., 2013). A few measurements have been performed on Arctic and European Alpine ice core samples with such optical methods (Doherty et al., 2010; Lavanchy et al., 1999). Recently, an incandescence method using single particle soot photometer (SP2, Droplet Measurement Technologies, Boulder, Colorado) was used to measure refractory BC (rBC) in ice cores. This term was coined because this technique is nearly independent of the morphology of BC and of the presence of other materials such as light-absorbing organics (Bisiaux et al., 2012a, 2012b; Kaspari et al., 2011; Jenkins et al., 2013; McConnell et al., 2007; Sterle et al., 2012). Its high sensitivity compared to other techniques makes it particularly suitable for measurements in snow and ice core samples from remote areas where BC concentrations are often low and the volume of sample is limited. However, the use of the SP2 technique for rBC measurements in snow and ice is not currently performed in the same way in the different studies and still raises many questions, ranging from the definition of calibration material to the process of aerosolization of rBC particles in melted snow and ice (Schwarz et al., 2012). Appropriate treatment of the samples is also required for accurate rBC analysis to minimize potential losses of rBC particles, as these are reported to easily adhere to the walls of the container due to their hydrophobic nature, and tend to form agglomerations with each other and/or with other particles including dust (Schwarz et al., 2012; Wang et al., 2012).

Many laboratory studies have reported that results of measurements of environmental carbonaceous particles depend not only on their source, and on the combustion process and mixing state, but also on the analytical techniques and experimental procedures used (Countess, 1990; Schmid et al., 2001). A recent review by Lack et al. (2014) describes the current state of BC measurement instrumentation, including the limitations and uncertainties of available techniques. In the past decade, several inter-laboratory studies reported that method inter-comparison can yield ambient EC estimates that differ by up to one order of magnitude (ten Brink et al., 2004; Schmid et al., 2001; Viana et al., 2007). These differences appear despite the good precision of each individual laboratory analysis and are attributed mainly to significant artifacts coming from organics present in the sample that pyrolize into char during the course of thermal analysis (Chow et al., 2001; Schmid et al., 2001; Cavalli et al., 2010). The ambient eBC provided by optical measurements can only be compared with EC (e.g., within a factor of 2 or less) when proper MAC values are used, and the values depend on the physical-chemical characteristics of the BC particles (Chow et al., 2009; Laborde et al., 2012). Otherwise, eBC : EC ratios can easily vary by more than a factor of three. The main factors responsible for the high variability of eBC : EC ratios are the amount of organics (e.g., refractory or water-soluble organic carbon) and dust, as well as the relative humidity of sampled air (Jeong et al., 2004; Yang et al., 2006). BC yields from the SP2 and several optical instruments were compared by Slowik et al. (2007) using laboratory-generated airbone BC particles. The measurements provided by the optical methods were ∼ 65 % higher depending on particle morphology and coating materials, whereas the SP2 output was independent of these particle characteristics. Another recent finding reported a small positive offset associated with dust content for the SP2 measurement, but which was much smaller than the positive artifact of the optical measurement (Schwarz et al., 2012). Recently, an inter-comparison study between a thermal-optical method, an optical method, and the SP2 measurements using a standard BC aerosol (airborne combustion aerosol standard, CAST soot, whose mass size distribution was within the detection range of the SP2) showed that measured rBC, EC, and estimated eBC mass concentrations were comparable at ∼ 10 % (Laborde et al., 2012). However, the detailed parameters involved in the determination of BC particles in those analyses are still not fully understood. This should ecourage further inter-comparison exercices. Such studies are even scarcer for snow or ice analyses. Only one inter-comparison study by Schwarz et al. (2012) between SP2 measurements and an optical method used snow sampled in semi-rural and rural areas. Given that rural and alpine aerosol samples exhibit even higher variances than urban aerosol samples in EC concentrations between analytical methods and laboratories, it is crucial to examine similarity/difference in BC particles in a variety of snow and ice samples according to different analytical methods. Furthermore, SP2 measurements and thermo-optical methods used to qualify rBC/EC in snow and ice have never been carefully compared, despite the observed discrepancy between rBC and EC concentrations even at the same Himalayan glacier site (e.g., Kaspari et al., 2011; Ming et al., 2008). The different terminology used in the different studies also contributes to some confusion and makes the comparison of studies somewhat difficult (Petzold et al., 2013).

In this paper, we describe and evaluate a methodology for rBC measurements in snow and firn samples using a SP2 technique that includes calibrating the SP2 with the most appropriate BC standard, building the coupling of nebulizer and SP2, and evaluating snow sample treatment methods. We compared the results of using this method with results using a thermal-optical method, Sunset OC-EC aerosol analyzer with the EUSAAR-2 protocol of Cavalli et al. (2010) using snow and firn samples from different locations.

2 Experimental

2.1 Measuring rBC in snow and ice samples with a Single Particle Soot Photometer

2.1.1 Principle of the SP2

The single particle soot photometer (SP2) uses a laser-induced incandescence method to measure the mass of individual rBC particles (Schwarz et al., 2006; Stephens et al., 2003) independently of particle morphology or of light scattering coating materials (Cross et al., 2010; Moteki and Kondo, 2010; Slowik et al., 2007). Individual rBC particles pass through the laser beam intra-cavity of a 1064 nm NdYAG laser adjusted to TEM_{00} mode with a Gaussian intensity distribution. The rBC particle absorbs light, reaches its vaporization temperature (~ 3700 to 4300 K) and incandesces while emitting visible radiation. The mass of individual rBC particle is proportional to its incandescence signal, as detected by two PMT-photo detectors with broad band (~ 350–800 nm) and narrow band (~ 630–800 nm) detection capabilities, respectively. The particle diameter is determined as a mass-equivalent diameter (MED) by assuming spherical morphology and an rBC particle density of $1.8\,\mathrm{g\,cm^{-3}}$. In our case, SP2 data were processed with the SP2 measurement toolkit developed by M. Gysel at the Paul Scherrer Institute (PSI, Switzerland).

2.1.2 Calibration of rBC mass in the SP2

The SP2 was calibrated by analyzing fullerene soot (Alfa Aesar Inc., USA), a standard BC material of known single particle mass aggregating primary particles with graphitic structure. Recent studies reported the similarity between the physical properties of fullerene soot and ambient rBC for urban areas in Switzerland and Tokyo (Laborde et al., 2012; Moteki and Kondo, 2010). The sizes of fullerene soot were selected by their electrical mobility diameter (D_{mob}) before entering the SP2 inlet by a differential mobility analyzer (DMA). The mass of mono-dispersed particles was empirically calculated using the relationship between the measured mobility diameter and the effective density of standard materials (Gysel et al., 2011; Moteki and Kondo, 2010). SP2 counts were validated by parallel measurements with a condensation particle counter (CPC). The number of concentrations obtained with both instruments agreed within 10 % in the calibration range.

The SP2 was calibrated for rBC mass using fullerene soot with a rBC mass ranging from ∼ 0.2 to 70 fg, corresponding to ∼ 70 to 420 nm MED. A quadratic spline fit curve applied to analyzed standard rBC masses was extrapolated to determine particles that were smaller and larger than the calibration range. The lower and upper limit of measurements for real rBC mass in actual samples was therefore ∼ 60–620 nm MED. The calibration size range generally covers ∼ 80–90 % of observed rBC mass in the SP2 detection range for the snow and firn samples tested (Sect. 2.3). Particles heavier than ∼ 220 fg (corresponding to ∼ 620 nm MED in rBC diameter) were detected by the SP2 but treated as if they had a BC mass of ∼ 220 fg due to the saturation of the A/D converters of the detectors. Note that the value 220 fg corresponds to a fullerene calibration, and the determined rBC mass and size at this saturation point might differ slightly depending on the calibration materials/curves. For all snow and firn samples tested in this study, underestimation of rBC mass concentration related to this instrument limitation was considered to be small, since the number of rBC particles detected at the saturation point represented < 0.1 % of the total number.

Calibration was performed regularly, specifically when the SP2 was moved, and calibration curves (for the high-gain output of the broadband incandescence channel) are reproducible within 4.5 % for fullerene soot. We used signals from the broad band detector for rBC particle detection, as it showed less noise and more stable calibration curves than the narrow band detector.

2.1.3 Aerosolization of rBC particles in liquid samples

Coupled to a nebulizer, the SP2 can be used to measure rBC mass concentration in liquid-phase samples. Aerosolization of rBC particles has been identified as one of the major uncertainties in determining total rBC mass concentration in liquid samples with the SP2 method (Ohata et al., 2011; Schwarz et al., 2012). Different types of nebulizing techniques have been used for ice core analysis. The SP2 has been coupled to an ultrasonic nebulizer (U5000AT, CETAC Technologies, Omaha, NE, USA) for rBC measurements of ice cores from Greenland (McConnell et al., 2007), Himalaya (Kaspari et al., 2011), and Antarctica (Bisiaux et al., 2012a), and for analysis of rain water (Ohata et al., 2011). When mentioned at all, the aerosolization efficiency of this ultrasonic nebulizer is often quite low (e.g., ~ 11 % in Ohata et al., 2011, and ~ 50 % in Kaspari et al., 2011) and its method of calibration is often not well described in detail in those ice core measurements. For the purpose of this study, we completed several aerosolization tests using both a jet nebulizer (APEX-Q, EPOND SA Corp., Switzerland) and the U5000AT.

Self-aspiration by a flow of compressed air of $1\,\mathrm{L\,min^{-1}}$ introduces the liquid sample in the APEX-Q nebulizer. Water droplets are then formed by the difference in pressure through a capillary of a concentric glass nebulizer. Particles are spun in the heated cyclonic spray chamber and liquid is desolvated in several heating (140 °C) and cooling (2 °C) steps, finally producing aerosols. The details of the U5000AT geometry and performance are described in previous studies (e.g., Ohata et al., 2011; Zanatta, 2012). The liquid sample flow rate is $70 \pm 10\,\mathrm{\mu L\,min^{-1}}$ for the APEX-Q, and $1.1\,\mathrm{mL\,min^{-1}}$ for the U5000AT nebulizer operated with a compressed air flow of $0.5\,\mathrm{\mu L\,min^{-1}}$. We derived the aerosolization efficiency of rBC particles through a nebulizer ($\mathrm{EF_{neb}}$) by the following:

$$\mathrm{EF_{neb}} = M_{\mathrm{SP2}} \cdot F_{\mathrm{neb.gas}} / (m_{\mathrm{samp}} \cdot \mathrm{F_{neb.liq}}) \qquad (1)$$

where M_{SP2} is the rBC mass concentration measured by the SP2 (µg cm^{-3}), $F_{neb.gas}$ is the air flow rate (cm^3 min^{-1}), m_{samp} is the rBC mass concentration of the injected sample (µg L^{-1}), and $F_{neb.liq}$ is the liquid flow rate of the sample (L min^{-1}).

From the repeated blank (Milli-$Q^{®}$, > 18.2 MΩ, 0.2 µm filtration) tests ($N > 10$ for both nebulizers), limits of detection (LOD, mean + 3σ of blank), limits of quantification (LOQ, mean + 10σ of blank) and coefficient of variation (CV, σ/mean × 100) were measured and were similar for both nebulizers, in the order of 0.01 µg L^{-1}, 0.03 µg L^{-1} and 70 %, respectively.

Full calibration of the coupling between the nebulizer and SP2, i.e. evaluation of aerosolization efficiency of the APEX-Q was performed with eight gravimetric standards, aquadag® in aqueous phase (ranging 0.1–100 µg L^{-1}) analyzed every two weeks. Over a ten-month period, and independently of concentration, 65 ± 4 % ($N = 20$, CV = 6 %) of rBC mass was recovered, assuming negligible mass of hydrogen and/or oxygen in the coating of the BC. The nebulizer-SP2 coupling was calibrated every day using the three standards of aquadag®, which also showed the same aerosolization efficiencies.

With the U5000AT, approximately 60–70 % of the sample volume is lost at the first drain before conversion to water droplets by the piezoelectric transducer. When the sample volume collected at the first drain is subtracted from the sample volume injected into the nebulizer, an aerosolization efficiency of 30 ± 3 % ($N = 4$, CV = 8 %) is observed. However, this approach may be unrealistic, as there is no evidence that rBC particles are homogeneously distributed between the first drain and the aerosols that are produced. Considering sample loss at the first drain, EF_{neb} of U5000AT of ~ 10 % was obtained, a value consistent with that reported in Ohata et al. (2011), although these authors operated the U500AT with a slightly different setting.

Figure 1 shows mass size distributions of aquadag® in water when nebulization was carried out with the APEX-Q and the U5000AT. Both distributions show a mass median diameter (MMD) of ~ 210–220 nm MED. For both nebulizers, the shape of size distribution was independent of aquadag® concentrations over the 0.1–100 µg L^{-1} range. Negligible amounts of rBC particles were measured at the saturation point of A/D converters of incandescence detectors with the U5000AT nebulizer, and this fraction was less than 0.1 % of total number of particles with the APEX-Q nebulizer. For ease of reading, data collected at this saturation point are not presented in Fig. 1. In fact, the analysis of the liquid removed at the first drain of the U5000AT revealed a larger MMD than in the original sample, confirming the lower efficency of this nebulizer for large particles. This finding is consistent with the results of a recent study by Schwarz et al. (2012) who demonstrated that U5000AT aerosolizes polystyrene latex sphere (PSL) particles larger than ∼ 500 nm with very poor efficiency (<∼ 10 %) in comparison with smaller particles. However, both nebulizers evaluated in this study had similar low detection limits (in the order of 0.01 µg L^{-1}) and slight variability (CV = 6–8 %).

The aerosolization efficiency observed with the APEX-Q was further confirmed by aerosolization of mono-dispersed PSLs with respective diameters of 203 nm and 240 nm, similar to MMD of aquadag®. The original concentrations reported by the manufacturer (Thermo scientific, USA) were measured by the SP2. We considered that PSLs were distributed homogeneously in the containers, and 70 ± 0 % ($n = 2$) and 79 ± 0 % ($n = 2$) of injected PSLs were aerosolized for diameters of 203 nm and 240 nm, respectively. We also assessed possible changes in rBC size distributions during aerosolization. Aerosol particles can collide due to their random motions and can coalesce to form larger chains of many particles. In fact, coagulated particles (detected when the mean diameter changes by ±20 %) only represented 2 ± 1 % and 1 ± 0 % of the total number of detected PSL particles of 203 nm and 240 nm, respectively. This result suggests that the coagulation effect of rBC particles is negligible in the APEX-Q, since coagulation frequency is considered to depend on the diameter and concentration of the particles (Jacobson et al., 1994). Therefore, the size distributions of aerosolized particles determined in the nebulizer can be considered to be representative of the original size distributions.

Finally, our study suggests that rBC losses during aerosolization depend on factors that are specific to each analytical system, underlining the crucial need for calibration. In this study, quantification of rBC losses during aerosolization, i.e. calibration of the nebulizer-SP2 coupling, was performed regularly (every two weeks) using eight aquadag® standards, and daily during each analytical session using three standards. The results were always within the range of 65 ± 4 %. The typical errors of $\mathrm{EF}_{\mathrm{neb}}$, M_{SP2}, $F_{\mathrm{neb.gas}}$, and $F_{\mathrm{neb.liq}}$ were estimated to be around 15 %, 10 %, 5 %, and 10 %, respectively, based on their repeated measurement, resulting in the overal uncertainty of about 20 %. Clearly, the higher aerosolization efficiency of APEX-Q compared with that of U500AT leads to lower uncertainty in rBC retrieval. Consequently, in the following, we used the SP2 in its APEX-Q configuration.

2.1.4 Repeatability and stability of SP2 analyses

The dependence of size distributions on sample concentrations was investigated with the coupled APEX-Q/SP2 system. The mass median diameter (MMD) and the count median diameter (CMD) of aquadag® obtained from lognormal fits were evaluated at different rBC concentrations ranging from 0.1 to 100 µg L^{-1}, i.e. the rBC concentrations frequently observed in snow and firn samples (see Table 2). Each measurement was made in triplicate using new standard solutions. The mean values of the MMD and the CMD were 220 and 67 nm MED for rBC concentrations ranging from 0.1 to 100 µg L^{-1}, resulting in a CV = 1.5 % and 0.6 %, respectively, confirming the reproducibility of our system for rBC size distirubitions over a wide range of rBC concentrations.

Different chemical species including ionic water-soluble species such as sulfate and calcium are included in solid precipitations (Preunkert et al., 2000; Savarino and Legrand, 1998) and thus coexist with rBC particles in deposited snow and ice. Aquadag® solutions spiked with water-soluble ionic species were also analyzed to investigate potential artefacts, since water-soluble species may affect the surface tension of droplets, and hence nebulizer efficiency (Facchini et al., 2000; Ohata et al., 2011).

To assess this effect in our system, we measured rBC concentrations of aquadag® solutions (10 µg L^{-1}) with 100–1000 ppb of sulfate and calcium, using five different concentrations. This range of sulfate and calcium covers the typical values in ice cores collected from the European Alpine region (Preunkert et al., 2000). The rBC concentrations in these artificial samples were stable within 8 % and 5 % without any trend for the aquadag® + sulfate samples and the aquadag® + calcium samples, respectively. Using the U5000AT-SP2 system, Ohata et al. (2011) also concluded that analytical errors due to possible changes in surface tension caused by such species are negligible, however, these authors mentioned that this may not be the the case for high concentrations of water-soluble humic-like substances (HULIS), e.g., > 100 mg L^{-1}. Typical water-soluble HULIS levels are below 50 ppbC in the Alpine ice core covering the 1920–2004 time period (Guilhermet et al., 2013). The impact of water soluble species on rBC particle aerosolization driven by change in water surface tension should thus benegligible.

2.2 Thermo-optical analysis of EC in snow and ice samples

One of the aims of this study was to compare SP2 and thermal-optical methods (Sect. 3.2). Briefly, the thermal-optical technique used for this comparison follows the EUSAAR (European Supersites for Atmospheric Aerosol Research)-2 protocol (Cavalli et al., 2010).

This protocol involves an OC-EC aerosol analyzer (Sunset laboratory Inc., US) that has been widely used for EC and OC analysis. The pre-heated quartz fiber filter loaded with particles is heated first in an oxygen-free ultra high purity helium atmosphere in increasing temperature steps, which allows for the detection of various organic carbon fractions. Then, the gas is switched to a 2 % O_2/He mixture and the filter is heated with increasing temperature steps for determination of EC. During the initial heating steps, some OC may undergo pyrolization (resulting in “pyrolyzed OC”) and be finally determined as EC due to EC-like light absorption. This pyrolytic conversion was continuously monitored and taken into account by measuring the transmission of a laser beam.

Since concentrations of EC and insoluble OC are low in snow and ice samples, a decarbonatation step is necessary for this type of samples. The detailed filtration and chemical decarbonation processes are presented in SI. Filtration with 100 mL of ultrapure water and a decarbonation procedure led to LODs of 4 µg C for OC and of 0.1 µg C for EC. Filtration with ultrapure water without decarbonatation showed the same detection limits, indicating that no contamination takes place during this process.

2.3 Origin of snow and ice samples used in the study

2.3.1 Alpine surface snow

Alpine snow samples were collected in September 2012 from the surface and from a 1.8 m deep snow pit at the Col du Dôme site (hereafter "CDD", 45°84′ N, 6°85′ E, 4270 m a.s.l.), located close to the summit of Mont Blanc (French Alps). We collected snow samples ($N = 46$) from the top 2 cm snow layer over an area of 0.8 m × 1.3 m over a period of one hour. In addition, snow samples were collected from the top 2 cm layer ($N = 5$) and from the top 5 cm layer ($N = 5$) in a neighboring area measuring 0.3 m × 1.9 m. The samples from the top 2 cm layer and from the top 5 cm layer were respectively stored in 50 mL and 125 mL polypropylene (PP) containers (VWR International), pre-rinsed with ultrapure water. The water equivalent volume of each snow sample was ∼ 10 mL and 30 mL for the 50 mL and 125 mL container, respectively. Snow was collected in one or two 1 L glass containers (Pyrex) from each layer of a four-layer snow pit. The snow pit was divided into layer 1 "fresh snow", layer 2 "summer layer", layer 3 "dust deposition", and layer 4 "winter layer". The collected samples were sealed in plastic bags, stored in a freezer, and kept frozen prior to analysis. The CDD surface snow and snow pit samples were used to optimize the snow and ice sample treatment method (Sect. 3.1) and to compare our SP2 method with the thermal-optical method of OC-EC aerosol analyzer (Sect. 3.2).

2.3.2 Caucasus high altitude firn

A 183 m ice core was drilled in September 2009 on Mt. Elbrus in the Caucasus (hereafter “ELB”, 43°20′ N, 42°25′ E, 5115 m a.s.l.). Five 1 m long firn sections from 9 to 14 m in depth were selected to compare our SP2 method with the thermal-optical method of OC-EC aerosol analyzer (Sect. 3.2). This is the first core from the Caucasus to be measured for rBC. Samples were from spring 2005 and spring 2007, and are affected by changes in both anthropogenic and natural aerosol emissions such as fossil fuel and biomass combustions and dust transport from arid areas. The core was kept frozen until analysis.

2.3.3 Greenland summit firn

A 305 m long ice core was drilled in July 1989 at Summit, central Greenland (hereafter “SUM”, 72°34′ N, 37°38′ W, 3240 m a.s.l.) as part of the European EUROCORE project. Three firn sections (29.2–30, 37.9–38.2 and 64.5–64.9 m) were analyzed in this study, covering multi-year periods over the last two centuries (corresponding to 1918–1922, 1893–1894 and 1799–1800 in calendar years, respectively). The sections contain records of historical changes in both anthropogenic and natural emissions of aerosol species in the high-latitude Northern Hemisphere (Savarino and Legrand, 1998). The samples were kept frozen prior to analysis. The firn samples were analyzed for the inter-comparison of two analytical methods (Sect. 3.2).

2.3.4 Himalayan surface snow

Surface snow was collected at high altitude sites in the Himalayan region in Nepal (hereafter “HIM”). The surface snow samples including fresh and old snows were collected at three sites, near the Nepal Climate Observatory-Pyramid station (NCO-P, 5079 m a.s.l.), the Changri Nup glacier (5644 m a.s.l.) and the Kongma glacier (5600 m a.s.l.) located in/near the Kumbu valley. All surface snow was sampled from the surface to a depth of 10 cm in 2010–2012. The snow was sampled somewhat randomly by time and/or location due to difficult access to the snowfields. Eleven samples were selected, depending on the volume of available samples or dust particle content. Eight snow samples collected in 1 L glass containers were tested for inter-instrumental comparison (Sect. 3.2). The other three samples collected in 100 mL glass containers with high dust concentrations were analyzed to investigate the impact of the settlement of dust particles (Sect. 3.2.3). Major sources of aerosols observed in the region have been identified as biofuel combustion and transported desert dust (Bonasoni et al., 2010; Decesari et al., 2009). These snow samples melted during transport and were consequently stored in the liquid phase in a fridge prior to analysis.

3 Results and discussion

A full evaluation and understanding of the method for the analysis of snow and ice samples with the SP2 technique is required before it can be compared with the thermal-optical method. Our discussion is thus organized along two axes: (i) how sample treatments can impact rBC analysis conducted with SP2 coupled with the APEX-Q nebulizer (Sect. 3.1), and (ii) which uncertainties should be considered when comparing rBC and EC data obtained with the two methods (Sect. 3.2).

3.1 Treatment of the snow and ice samples before SP2 analysis

Natural freeze/thaw cycles within snow packs that affect the size and shape of snow grains (Dominé et al., 2003) may also affect the properties of rBC particles (e.g., Flanner et al., 2012). The rBC particles can undergo physical changes during melting/re-freezing processes in sample containers, depending on the procedure used to transport the samples from the field and their conservation. Recently, Schwarz et al. (2012) tested the effects of snow sample acidification, agitation, and storage on rBC mass and size determinations. Nevertheless, the detailed complete evaluation of snow sample treatment prior to SP2 analysis is still necessary.

A series of tests using the natural CDD snow samples were performed to identify the optimal sample treatment to minimize losses of rBC particles and changes in their size distributions. We investigated the variability of rBC concentrations in snow samples from the top 2 cm ($N = 51$) and the top 5 cm ($N = 5$) layers by direct measurements without pre-treatment. All the samples had comparable rBC concentration with CV of 18 % and 17 %, respectively, indicating that they could be used for this comparison study. The mean of the top 2 cm samples ($N = 5$) in the 0.3 m × 1.9 m area was very similar to that in the 0.8 m × 1.3 m area ($N = 46$), with values only 3 % higher.

The CDD snow was thus treated using different methods and subsequently analyzed with the SP2. We specifically investigated the impact of container condition, melting procedure, multiple melting/freezing cycles, the surface-to-volume ratio of the sample container, and storage procedures after melting.

3.1.1 Choice of sample containers

We first tested the widely used PP containers as snow sample containers. Blanks were in new PP containers pre-rinsed with ultrapure ultrapure water with/without 15 min sonication. Blank rBC levels under both sonication conditions were $< 0.01\,\mu\text{g L}^{-1}$ based on repeated analyses. Blank levels of $\sim 0.05\,\mu\text{g L}^{-1}$ were found after sonication for 30–45 min, but were still much lower than the lower limit of field snow or ice sample level, i.e. $\sim 0.1\,\mu\text{g L}^{-1}$. Thus, all new PP containers were only pre-rinsed with ultrapure water before sampling. Conversely, recycled glass containers stored filled with ultrapure water, without cleaning by sonication, were found to be significantly contaminated by rBC particles from previous samples. Blank levels of pre-rinsed glass containers ($N = 8$) ranged between 0.1 and $12\,\mu\text{g L}^{-1}$ without sonication and $\sim 0.01\,\mu\text{g L}^{-1}$ with 15 min sonication. This suggests potentially significant contamination of the following samples when sample-filled glass containers are sonicated without proper cleaning beforehand. They reached the blank level of $< 0.01\,\mu\text{g L}^{-1}$ only after being cleaned with ultrapure water with intense sonication (30 min). Consequently, if sonication of the samples is necessary, recycled glass containers should be cleaned by 30 min sonication with ultrapure water to avoid contamination of subsequent samples. In addition, a previous study (Zanatta, 2012) reported of PP containers had a less absorptive and more stable surface than glass containers made by the same manufacturer and the same model by testing linearity and reproducibility of standard BC in water. As a result, we mainly used PP containers in this study, as low blank values are more easily and more consistently obtained with these containers.

3.1.2 Effect of melting procedures

Previous studies involving measurements of rBC or EC in snow and ice samples did not use standardized sample melting methods. For example, snow or ice was thawed at room temperature (Jenk et al., 2006; Lavanchy et al., 1999; Thevenon et al., 2009; Wang et al., 2012); snow was melted in a warm bath ($< 30\,^{\circ}$C) (Ming et al., 2008) or in a microwave oven (Schwarz et al., 2012); or ice was melted into discrete samples using a continuous melter system (Kaspari et al., 2011).

In this work, we tested two melting procedure whose results are listed in Table 1a. The CDD snow stored in 50 mL PP containers was (i) melted at room temperature for less than 2 h, or (ii) melted in a warm water bath at 30 °C for less than 20 min. Mechanical stirring during melting was not used as we observed that it did not cause any distinct change in rBC concentration, in agreement with results of a study by Schwarz et al. (2012). Samples melted in a warm bath did not show a significant difference in rBC concentration compared to samples melted at room temperature, i.e. there was only a $3 \pm 9\,\%$ increase. To investigate potential rBC losses during melting, all the samples were measured a second time after 15 min sonication. No changes in rBC concentrations were observed before and after sonication in samples initially melted at room temperature. The samples melted in a warm bath exhibited a slight increase ($12 \pm 18\,\%$) in rBC concentration after sonication, which we did not consider to be critical due to a relatively larger standard deviation for the smaller number of samples ($N = 10$).

These results showed that melting samples at room temperature in less than 2 h caused no additional rBC losses compared to melting in an warm bath for a shorter time, i.e. in less than 20 min, despite that the fact it is generally thought that faster melting leads to fewer rBC particle losses. Sample treatment with sonication is also unnecessary when samples are melted rapidly (i.e. in less than 2 h). However, rapid melting in a warm bath or applying sonication after melting does not cause significant differences compared to more straightforward melting at room temperature without sonication.

3.1.3 Effect of multiple melting/freezing/melting cycles

Re-freezing/melting processes may lead to the redistribution of particles in a sample container (e.g., particles sticking to the wall of the container). To simulate a melting/freezing/melting cycle, snow samples were re-frozen immediately after analysis and then re-melted at room temperature for less than 2 h prior to a second analysis. Interestingly, there was a marked decrease in rBC concentrations during this process (45 ± 11 %, Table 1b). We thus suggest that the observed loss of rBC particles happened during freezing of the sample, as we previously demonstrated that melting had no impact if conducted within 2 h (Table 1a). The re-melted samples were then treated using different methods to investigate rBC recovery after freezing ($N = 5$ for each method, Table 1b): ultra-sonication (for 15 min, 30 min and 45 min), and acidification. rBC losses of 38 ± 16 % were still recorded after 15 min sonication, but decreased to 14 ± 14 % after 30 min sonication. Sonification for 45 min was no more efficient. Thirty minutes of sonication led to the highest rBC recovery rate observed after a freezing/re-melting cycle. In addition, the tested samples ($N = 3$) were re-frozen, re-melted (thus, artificially re-frozen two times in total) and analyzed, which showed rBC total mass reduction of ~ 50–70 % and 30 min sonication helped only ~ 10 % increase in rBC mass concentration. We observed significant rBC losses over all size ranges in the re-melted samples and the lost rBC particles were recovered uniformly over almost all size ranges after 30 min sonication. We also acidified samples with 0.5 M nitric acid, following the procedure described by Kaspari et al. (2011). Acidification did not reduce losses of rBC after a freezing/re-melting cycle (0 % variation).

3.1.4 Effect of the surface-to-volume ratio of sample containers

The surface-to-volume (S/V) ratio of sample containers may affect rBC losses that occur during a melting/freezing cycle. This concern arose because our main assumption concerning rBC losses in a container is particles adhering on the wall of the container. Two types of PP containers with different S/V ratios were used to test this hypothesis: a 50 mL PP tube container with $S = 22.9\,\text{cm}^2$ and $V = 10$ mL of the samples ($N = 5$, $S/V = 2.3\,\text{cm}^2\,\text{mL}^{-1}$), and a 125 mL cylindrical PP container with $S = 75.4\,\text{cm}^2$ and $V = 30$ mL of the samples ($N = 5$, $S/V = 2.5\,\text{cm}^2\,\text{mL}^{-1}$). The 125 mL containers had a 10 % larger S/V than the 50 mL containers. After refreezing/melting, average rBC mass losses from the two containers were 37 ± 14 % and 55 ± 30 %, respectively (Table 1c). After 30 min sonification, rBC losses from the 125 mL container were still 41 ± 34 %, while more particles were recovered from the 50 mL containers, with rBC losses of only 11 ± 26 %. This result highlights the fact that a difference of only 10 % in the S/V ratio can influence rBC losses during cycles of refreezing/melting.

3.1.5 Effect of storage procedures after melting

Snow samples stored in PP containers were first analyzed without treatment (e.g., sonication or acidification) and stored at room temperature (5–15 °C) or in a refrigerator (4.5 °C) to evaluate rBC losses as a function of time. These samples were analyzed 2 h, 4 h, 6 h and 24 h after the first melt cycle, without any additional treatment. Changes in mean rBC concentrations were not significant in the samples maintained at room temperature, but their concentrations were more variable than in samples kept in the refrigerator (Table 1d). However, after 24 h at room temperature, the change in rBC concentrations was slight (−9 ± 17 %), particularly compared to the rBC losses during refreezing/melting.

When rBC concentrations were monitored in samples stored in glass containers at room temperature for 24 h, similar results were observed. Schwarz et al. (2012) also mentioned that rBC losses in glass containers stored at room temperature were limited, although they showed that losses were higher (about 50 %) in high-density polyethylene bottles. The difference between their results and ours might be due to the storage temperature and/or to the rBC concentrations, which differed from ours.

rBC mass losses from melted snow samples kept in the refrigerator remained constant for 24 h with −3 ± 6 % change. The same snow samples were kept in the refrigerator for a week and rBC was then analyzed again. Changes in rBC masses after a week were −13 % on average, a value that was reduced to −7 % after 15 min sonication. Sonication thus helps recover rBC particles in samples stored in the liquid phase for more than one day.

3.1.6 Summary

According to the series of tests described in Sect. 3.1, we recommend the following method to minimize a reduction in rBC concentrations and changes in associated rBC size distributions when measuring snow or ice samples.

- Samples should ideally be stored in new polypropylene (PP) containers, which are pre-rinsed with ultrapure water. The container should have the smallest possible surface-to-volume ratio. Recycled glass containers should be cleaned by intense sonication (30 min), especially if samples need to be sonicated before analysis.
- Melting should be rapid (e.g., < 2 h), in which case additional treatments such as sonication are not necessary. Re-freezing samples should be avoided. Re-melted samples showed rBC mass losses of −45 ± 11 % in 50 mL PP containers. If samples are melted either partially or entirely, sonication for more than 30 min

is recommended. After 30 min sonication, the rBC mass losses were reduced by a factor of ∼ 3.

- If samples have to be kept in the liquid phase for a few hours prior to analysis, storing them for one day in a refrigerator or at room temperature will not lead to serious rBC losses (< 10 %). However, storing the samples in the refrigerator was found to be more stable and likely less problematic.

3.2 Comparison between the SP2 and thermal-optical methods

Inter-comparison of the SP2-based and thermal optical methods has already been carried out for atmospheric BC samples (e.g., Countess, 1990; Jeong et al., 2004; Laborde et al., 2012; Schmid et al., 2001; Yang et al., 2006). Similar studies for rBC measurements in snow and ice samples are still very rare (e.g., Schwarz et al., 2012). Here, we report the results of a comparison between our SP2 method (Sects. 2.1 and 3.1) and the thermal-optical method of Sunset OC-EC aerosol analyzer operated using the EUSAAR-2 protocol (Sect. 2.2). Snow and firn of various origins were used to better characterize the limitations of the two approaches. Specifically, SUM and ELB firn, and CDD and HIM snow (see Sect. 2.3) were analyzed with both SP2 and the OC-EC Sunset analyzer.

Considering their large volume in 1 L glass containers, snow and firn were melted in a warm bath to minimize melting time. Only the HIM snow was sonicated for 15 min to avoid rBC particle loss on the container walls since they had been stored in the liquid phase. The melted samples were filtrated and split into aliquots for immediate rBC analysis by the SP2 (10 mL PP) and dust analysis by a Coulter Counter Multisizer (10 mL accuvette) (Multisizer™ 3 COULTER COUNTER®, Beckman Coulter, Inc, USA) in a 100 class clean room. Filtration was carefully performed using the method described in SI. EC and rBC concentrations and EC : rBC ratios are listed in Table 2. Note that all rBC data were corrected for losses during the aerolization processes through daily calibration (see Sect. 2.1.3). The EC : rBC ratio was 1.8 ± 1.2 for the SUM, 0.4 ± 0.2 for the CDD, 0.9 ± 0.3 for the ELB, and 3.0 ± 1.2 for the HIM samples.

We observed significant differences between the two techniques with EC : rBC ratios ranging from 0.4 to 3.0 depending on the origin of the snow and firn. This obviously poses a number of problems in interpreting BC in ice cores. In the following, we discuss the artifacts that could have led to these discrepancies between the two techniques.

3.2.1 rBC artifact from aerosolization calibration due to size-shifted rBC

Since size distributions of BC particles mainly depend on their emission sources and coagulation processes, their sizes range from a few nanometers to a few micrometers (Bond et al., 2013). As mentioned in Sect. 2.1.2, the SP2 provides rBC particle size distribution between ~ 60–620 nm MED, but particles larger than 620 nm MED are considered by the analyzer to be particles with a diameter of 620 nm (detector saturation). Underestimation of > 620 nm rBC particles may thus be an issue. Recently, Schwarz et al. (2012) reported the rBC size distributions of rural/semi-rural snow showing significant rBC mass contributions at larger sizes than in typical ambient air (where > 90 % of rBC mass is below 600 nm volume equivalent diameter, VED). In our case, however, less than 0.1 % of the total number of rBC particles in all the samples we tested was found at the saturation point. In particular, the contribution of rBC at saturation point (620 nm) in the SUM and CDD samples represented less than 0.05 % of total rBC. For the high altitude snow and firn tested in the study, the contribution of larger particles above the detection range of our SP2 appeared to be very small, probably due to the long distance from the source.

However, gravimetric calibration assumes that rBC particles have similar size distributions in standards and in field samples. Mass size distributions of rBC in snow and firn samples are plotted in Fig. 2. For most of the SUM, CDD, and ELB samples, rBC mass contribution of each size bin to total mass concentration are very similar to the size distributions of aquadag® (Fig. 2). By contrast, the HIM samples showed a significant shift towards the larger size compared to aquadag®. In such cases, our method of calibration would not be suitable for the analyzed samples. Considering the highest EC : rBC ratios found in the HIM samples (3.0 ± 1.2, Table 2), the shift of particle size distributions between samples and standard solutions likely contributed to underestimation of rBC concentrations. Quantification of such rBC underestimation is not possible only using SP2. However, it should be noted that our choice of calibration material (i.e., aquadag® solutions) was appropriate for the other snow and firn samples

3.2.2 EC artifact due to inadequate filtration

To our knowledge, there is no size-limitation in the thermal-optical method, which can theoretically analyze all EC particles on the filter. However, the sample filtration step may involve EC losses especially of fine particles that can pass through the filter with the sample water. EC losses that occurred during filtration of sample water were investigated by Ducret and Cachier (1992) and Lavanchy et al. (1999). Overall, these authors concluded that collection efficiency was almost 95 %. We performed similar tests to determine filtration efficiency using the SP2 method and focusing on fine mode particles. The efficiency of sample filtration through the quartz fiber filter (FE) was evaluated by SP2 analysis of samples before and after filtration. Thus:

$$\mathrm{FE} = 1 - \frac{\text{rBC in sample after filtration}}{\text{rBC in sample before filtration}} \tag{2}$$

Table 2 lists the filtration efficiency of the four types of sample analyzed, with values ranging from 30 % to 90 %. All the samples showed a significant fraction of rBC that was not retained on the filter during filtration, and consequently not measured by the thermal-optical method. In particular, only ∼ 30–40 % of rBC mass in CDD snow samples was retained by the quartz filter. A significant fraction of rBC particles <∼ 200 nm MED passed through the filter (Fig. S2). This was confirmed in the CDD samples by electron microscopy of the second filtrated liquid on a 0.2 µm nuclepore after filtration using quartz filters. The presence of BC aggregates with diameters ranging between

100 and 200 nm are frequently visible in microscopy images, contrary to larger BC particles (Fig. S3). In contrast, we observed a much higher filtration efficiency for the HIM with FEs ranging from 70 % to 90 %. This can probably be attributed to the adsorption of BC particles onto existing dust particles, which artificially shifts the BC to larger sizes and hence increases filtration efficiency.

ELB and SUM samples showed intermediate filtration efficiencies (∼ 40–60 %). Like HIM samples, the presence of OC or dust may increase rBC on the quartz filter by adsorption. Although the concentrations of OC and dust in the SUM samples were low, we had used much larger filtration volumes (∼ 1–2 L) making their OC loading 2–10 times higher than for CDD and ELB samples (Table 2). We conclude that both total loading of OC and dust on a quartz filter can affect how a quartz filter retains BC, and hence BC quantification performed with the Sunset analyzer. Consequently, previous snow and ice studies that reported concentrations of EC filtrated using quarz filters may have underestimated EC concentration by a significant but as yet unquantifiable factor. This would be the case for EC measurements using a quarz fiber filter for the Arctic and Alpine snow and ice performed for example by Hagler et al. (2007), Lavanchy et al. (1999), Ming et al. (2008, 2009) or Thevenon et al. (2009).

3.2.3 Artifact due to the presence of dust

Apart from their impact on filtration efficiency (see 3.2.2), high levels of dust in liquid samples may affect both rBC and EC determinations (Schwarz et al., 2012; Wang et al., 2012). We first investigated the impact of dust on the SP2-based rBC analysis by simply allowing dust particles to settle before sampling for SP2 measurements. This was done using HIM snow samples with a high level of dust ($N = 3$, dust concentration of ∼ 50 ppm). We compared rBC concentrations at regular intervals for 15 min without stirring the sample. The rBC concentrations ranged between ∼ 35 and 70 $\mu g L^{-1}$, and remained constant at around 5 %. Although a small positive offset of dust content for the SP2 measurement was reported previously (Schwarz et al., 2012), which was around +15 $ng g^{-1}$ offset in the snow sample with dust concentration of ∼ 50 ppm, the potential positive artifact was only ~ 1–3 µg L^{-1} in the snow samples with dust concentration of ~ 50 ppm in our study. Considering high mass ratios of dust to rBC of ~ 1000 in these samples, dust and rBC particles were likely agglomerated (Wang et al., 2012). However, this did not significantly affect rBC concentrations and we thus conclude that the impact of dust on SP2 detection is not significant in such case.

On the other hand, the presence of dust affected the Sunset analysis, independently of issues related to sample filtrations. The impact of dust on thermal-optical method has been addressed in previous laboratory studies (e.g., Chow et al., 2001; Elmquist et al., 2006; Fung, 1990; Wang et al., 2012). Dust particles including catalytically active ions or mineral oxides (e.g., hematite) can reduce the sensitivity of the instrument (Chow et al., 2001) but also bias the OC/EC split point during the analysis by delaying or preventing the laser signal from reaching its initial value (Elmquist et al., 2006; Fung, 1990; Wang et al., 2012). Consequently, EC concentrations of dusty samples are generally underestimated or not determined. In this study, however, we observed a lack of a systematic correlation between EC and dust concentration.

The thermograms of OC-EC analysis of the dusty CDD snow layer 2 and 3 (dust of ~ 1 ppm and 10 ppm, respectively) reveal such artifacts. The laser signal did not return to the its baseline value before the end of analysis, resulting in no EC fraction. The yellowish or dark-brown color of these snow samples changed to red-brown after combustion, indicating the existence of hematite. To eliminate the impact of dust on incomplete OC/EC splitting, the results were revised following procedures described by Wang et al. (2012). It should be noted that this revision was somewhat rough as we did it by visually modifying the initial reflectance value line in the thermograms, but the revised EC concentrations are comparable to rBC concentrations. These revised concentrations are listed in Table 2. Interestingly, we did not always observe artifacts on Sunset thermograms when we analyzed highly dusty samples from other sites (e.g. HIM samples with a dust concentration of ~ 50 ppm). Consequently, we conclude that not only the concentration but also the type of dust can lead to analytical failure in EC measurements. Finally, our results suggest that elevated dust content does not

Title Page
Abstract | Introduction
Conclusions | References
Tables | Figures
◂◂ | ▸▸
◂ | ▸
Back | Close
Full Screen / Esc
Printer-friendly Version
Interactive Discussion

have a clear impact on rBC measurement with the SP2, but we recommend systematic evaluation of the thermogram during EC analysis, particularly if the sampling site is influenced by local or regional dust sources.

3.2.4 EC artifact due to OC pyrolization

OC pyrolysis, which occurs during thermal-optical EC detection, could affect EC determination by biasing the OC/EC split point and then generally causing a positive EC artifact, if not properly corrected (Chow et al., 2001; Schmid et al., 2001). The snow and firn samples we tested included 40 % ($N = 8$) out of a total of 20 in which the pyrolyzed OC fraction represented half the total OC, i.e., pyrolized_OC/total_OC ratio ≥0.5, which is rarely observed in atmospheric samples in French urban sites (unpublished data). We selected samples with pyrolized_OC/total_OC ratio ≥0.5 ($N = 8$) and illustrate the relationship between pyrolized_OC/total_OC ratio and EC concentration in Fig. 3. The EC concentration generally increased with an increase in the pyrolized_OC/total_OC ratio, with a Pearson correlation coefficient (r^2) of 0.5 (p value < 0.01). Conversely, no linear relationship of Pyrolized_OC/total_OC ratio and rBC concentration was observed for these samples ($r^2 < 0.1$). The sampling sites containing the highest sample numbers included in Fig. 3 were ELB and HIM. In fact, ELB and HIM samples showed the highest OC concentrations (369 ± 61 $\mu g\,L^{-1}$ and 359 ± 185 $\mu g\,L^{-1}$, respectively), whereas OC concentrations in SUM and CDD samples were much lower (Table 2). Previous studies reported that some non-volatile OC fractions are prone to pyrolysis during thermal analysis, these being OC with high molecular weight (Miyazaki et al., 2007; Yu et al., 2004) or HULIS (Cavalli et al., 2010; Clarke et al., 2007; Kondo et al., 2011). We cannot confirm which organic fractions underwent pyrolysis in our samples. However, this result clearly suggests that the higher pyrolyzed OC fraction causes a positive EC artifact in the snow and firn samples probably by biasing the OC/EC split point, and consequently leading a fraction of pyrolyzed OC to be determined as EC.

We observed lower OC concentrations in SUM samples ($N = 3$) than in ELB and HIM samples, but the large volumes of SUM samples filtered for EC analysis meant that a higher OC mass was loaded on the filter in the case of SUM samples (143 ± 83 µg). The SUM samples generally showed a positive relationship between pyrolized_OC/total_OC ratio and both (i) OC mass loading on the filter and (ii) the sample volume filtered. We consequently suggest that the high EC : rBC ratio of 1.8 ± 1.2 observed in the SUM samples may be partially and indirectly explained by the large sample volumes used. This means that appropriate sample volumes should be carefully chosen and applied during EC filtration for thermal-optical analysis to reduce potential uncertainties.

4 Conclusions

We evaluated a rBC measurement methodology coupling jet nebulizer (APEX-Q) and SP2, through an extended series of tests using both rBC standard material and various types of snow and firn collected from different glaciers worldwide. The SP2 was calibrated with fullerene soot. We used aquadag® solutions only for the calibration of liquid-phase analysis by coupling nebulizer and SP2. We showed that aerosolization is more efficient with APEX-Q than with U5000AT nebulizer, with 65 ± 4 % and 30 ± 3 % efficiency, respectively, when sample losses at the first drain were not considered for the U500AT. APEX-Q led to better aerosolization of large rBC particles with a much smaller sample volume. To avoid potential rBC losses and changes in rBC size distribution of snow and ice samples, we propose a series of recommendations concerning the choice of container, first melting of the sample, melting/freezing/melting cycles, surface-to-volume ratio of the sample container, and storage. These sample treatment methods could also be used for the determination of EC using thermal methods. The comparison between the SP2 and the thermal-optical (Sunset OC-EC aerosol analyzer with EUSAAR-2 protocol) methods was carried out at the optimized set-up of each method, and their potential artifacts were investigated. This inter-comparison was conducted with four different types of samples: Greenland summit firn core (SUM), surface snow layers from the French Alpine region (CDD), firn from the Caucasus region (ELB), and

Himalayan surface snow (HIM). We observed significant differences between EC and rBC, which were not constant in the different samples. The EC : rBC ratio was 1.8 ± 1.2 for SUM, 0.4 ± 0.2 for CDD, 0.9 ± 0.3 for ELB, and 3.0 ± 1.2 for HIM.

The observed difference in the concentration of rBC and EC in the snow and firn samples is related to the complexity of artifacts in both methods. The variability of EC : rBC ratio can first be attributed to inadequate gravimetric correction of rBC aerosolization using aquadag® for samples exhibiting a different size distribution than that of aquadag®. Coupling the APEX-Q nebulizer and the SP2 analyzer can provide an optimized method with no significant bias for accurate measurements of rBC mass concentrations and size distributions in snow and ice samples. However, we recommend first checking if the rBC size distributions of the samples and calibrating material are sufficiently similar to ensure correct calibration of aerosolization This was the case for the HIM samples in our study when a shift of rBC particles toward larger sizes likely made our aerosolization correction incomplete, thus contributing to underestimation of rBC with the SP2 and leading to high EC : rBC ratios. More important, our results highligh quite significant EC artifacts related to low filtration efficiency (i.e., ∼ 30–90 %) of rBC particles on quartz fiber filters. This low particle collection rate was tightly linked to BC size distributions, filtered sample volumes, and the presence of elevated levels of OC and dust on the filters. Other artifacts such as the effect of dust or of the pyrolized OC fraction on the OC/EC split point should also be taken into consideration when using the thermal-optical method. Overall, we advise careful assessment of the analytical methods and procedures with respect to the characteristics of the samples concerned.

Supplementary material related to this article is available online at http://www.atmos-meas-tech-discuss.net/7/3549/2014/amtd-7-3549-2014-supplement.pdf.

Acknowledgements. This work was supported by the EU FP7 IP PEGASOS (FP7-ENV-2010/265148), the French ANR programs RPD COCLICO (ANR-10-RPDOC-002-01), PAPRIKA (ANR-09-CEP-005-02) and LABEX OSUG@2020. Support was also supplied by the Korean Ministry of Education and Science Technology through a government scholarship for S. Lim. We thank M. Legrand and S. Preunkert for many helpful discussions and lab assistance. We are also grateful to B. Jourdain and LGGE colleagues for field support at Col du Dôme, V. Mikhalenko and S. Kutuzov for providing Elbrus firn samples, and colleagues from EvK2 (CNR) for collection of the Himalayan snow samples.

References

Aamaas, B., Bøggild, C. E., Stordal, F., Berntsen, T., Holmén, K. I. M., and Ström, J.: Elemental carbon deposition to Svalbard snow from Norwegian settlements and long-range transport, Tellus B, 63, 340–351, doi:10.1111/j.1600-0889.2011.00531.x, 2011.

Bisiaux, M. M., Edwards, R., McConnell, J. R., Albert, M. R., Anschütz, H., Neumann, T. A., Isaksson, E., and Penner, J. E.: Variability of black carbon deposition to the East Antarctic Plateau, 1800–2000 AD, Atmos. Chem. Phys., 12, 3799–3808, doi:10.5194/acp-12-3799-2012, 2012a.

Bisiaux, M. M., Edwards, R., McConnell, J. R., Curran, M. A. J., Van Ommen, T. D., Smith, A. M., Neumann, T. A., Pasteris, D. R., Penner, J. E., and Taylor, K.: Changes in black carbon deposition to Antarctica from two high-resolution ice core records, 1850–2000 AD, Atmos. Chem. Phys., 12, 4107–4115, doi:10.5194/acp-12-4107-2012, 2012b.

Bonasoni, P., Laj, P., Marinoni, A., Sprenger, M., Angelini, F., Arduini, J., Bonafè, U., Calzolari, F., Colombo, T., Decesari, S., Di Biagio, C., di Sarra, A. G., Evangelisti, F., Duchi, R., Facchini, MC., Fuzzi, S., Gobbi, G. P., Maione, M., Panday, A., Roccato, F., Sellegri, K., Venzac, H., Verza, GP., Villani, P., Vuillermoz, E., and Cristofanelli, P.: Atmospheric Brown Clouds in the Himalayas: first two years of continuous observations at the Nepal Climate Observatory-Pyramid (5079 m), Atmos. Chem. Phys., 10, 7515–7531, doi:10.5194/acp-10-7515-2010, 2010.

Bond, T. C., Doherty, S. J., Fahey, D. W., Forster, P. M., Berntsen, T., DeAngelo, B. J., Flanner, M. G., Ghan, S., Kärcher, B., Koch, D., Kinne, S., Kondo, Y., Quinn, P. K., Sarofim, M. C., Schultz, M. G., Schulz, M., Venkataraman, C., Zhang, H., Zhang, S., Bellouin, N., Guttikunda, S. K., Hopke, P. K., Jacobson, M. Z., Kaiser, J. W., Klimont, Z., Lohmann, U., Schwarz, J. P., Shindell, D., Storelvmo, T., Warren, S. G., and Zender, C. S.: Bounding the role of black carbon in the climate system: a scientific assessment, J. Geophys. Res.-Atmos., 118, 5380–5552, doi:10.1002/jgrd.50171, 2013.

Cavalli, F., Viana, M., Yttri, K. E., Genberg, J., and Putaud, J.-P.: Toward a standardised thermal-optical protocol for measuring atmospheric organic and elemental carbon: the EUSAAR protocol, Atmos. Meas. Tech., 3, 79–89, doi:10.5194/amt-3-79-2010, 2010.

Chow, J. C., Watson, J. G., Crow, D., Lowenthal, D. H., and Merrifield, T.: Comparison of IMPROVE and NIOSH Carbon Measurements, Aerosol Sci. Tech., 34, 23–34, doi:10.1080/02786820119073, 2001.

Chow, J. C., Watson, J. G., Doraiswamy, P., Chen, L.-W. A., Sodeman, D. a., Lowenthal, D. H., Park, K., Arnott, W. P., and Motallebi, N.: Aerosol light absorption, black carbon, and elemental carbon at the Fresno Supersite, California, Atmos. Res., 93, 874–887, doi:10.1016/j.atmosres.2009.04.010, 2009.

Clarke, A. D. and Noone, K. J.: Soot in the Arctic snowpack: a cause for perturbations in radiative transfer, Atmos. Environ., 19, 2045–2053, doi:10.1016/0004-6981(85)90113-1, 1985.

Clarke, A. D., McNaughton, C., Kapustin, V., Shinozuka, Y., Howell, S., Dibb, J., Zhou, J., Anderson, B., Brekhovskikh, V., Turner, H., and Pinkerton, M.: Biomass burning and pollution aerosol over North America: organic components and their influence on spectral optical properties and humidification response, J. Geophys. Res., 112, D12S18, doi:10.1029/2006JD007777, 2007.

Countess, R. J.: Interlaboratory analyses of carbonaceous aerosol samples, Aerosol Sci. Tech., 12, 114–121, doi:10.1080/02786829008959331, 1990.

Cross, E. S., Onasch, T. B., Ahern, A., Wrobel, W., Slowik, J. G., Olfert, J., Lack, D. a., Massoli, P., Cappa, C. D., Schwarz, J. P., Spackman, J. R., Fahey, D. W., Sedlacek, A., Trimborn, A., Jayne, J. T., Freedman, A., Williams, L. R., Ng, N. L., Mazzoleni, C., Dubey, M., Brem, B., Kok, G., Subramanian, R., Freitag, S., Clarke, A., Thornhill, D., Marr, L. C., Kolb, C. E., Worsnop, D. R., and Davidovits, P.: Soot particle studies – instrument inter-comparison – project overview, Aerosol Sci. Tech., 44, 592–611, doi:10.1080/02786826.2010.482113, 2010.

Decesari, S., Facchini, M. C., Carbone, C., Giulianelli, L., Rinaldi, M., Finessi, E., Fuzzi, S., Marinoni, A., Cristofanelli, P., Duchi, R., Bonasoni, P., Vuillermoz, E., Cozic, J., Jaffrezo, J. L., and Laj, P.: Chemical composition of PM_{10} and PM_1 at the high-altitude Himalayan station Nepal Climate Observatory-Pyramid (NCO-P) (5079 m a.s.l.), Atmos. Chem. Phys., 10, 4583–4596, doi:10.5194/acp-10-4583-2010, 2010.

Doherty, S. J., Warren, S. G., Grenfell, T. C., Clarke, A. D., and Brandt, R. E.: Light-absorbing impurities in Arctic snow, Atmos. Chem. Phys., 10, 11647–11680, doi:10.5194/acp-10-11647-2010, 2010.

Dominé, F., Lauzier, T., Cabanes, A., Legagneux, L., Kuhs, W. F., Techmer, K., and Heinrichs, T.: Snow metamorphism as revealed by scanning electron microscopy., Microsc. Res. Techniq., 62, 33–48, doi:10.1002/jemt.10384, 2003.

Ducret, J. and Cachier, H.: Particulate carbon content in rain at various temperate and tropical locations, J. Atmos. Chem., 15, 55–67, doi:10.1007/BF00053609, 1992.

Facchini, M. C., Decesari, S., Mircea, M., Fuzzi, S., and Loglio, G.: Surface tension of atmospheric wet aerosol and cloud/fog droplets in relation to their organic carbon content and chemical composition, Atmos. Environ., 34, 4853–4857, 2000.

Flanner, M. G., Zender, C. S., Randerson, J. T., and Rasch, P. J.: Present-day climate forcing and response from black carbon in snow, J. Geophys. Res., 112, D11202, doi:10.1029/2006jd008003, 2007.

Flanner, M. G., Liu, X., Zhou, C., Penner, J. E., and Jiao, C.: Enhanced solar energy absorption by internally-mixed black carbon in snow grains, Atmos. Chem. Phys., 12, 4699–4721, doi:10.5194/acp-12-4699-2012, 2012.

Ginot, P., Dumont, M., Lim, S., Patris, N., Taupin, J.-D., Wagnon, P., Gilbert, A., Arnaud, Y., Marinoni, A., Bonasoni, P., and Laj, P.: A 10 yr record of black carbon and dust from Mera Peak ice core (Nepal): variability and potential impact on Himalayan glacier melting, The Cryosphere Discuss., 7, 6001–6042, doi:10.5194/tcd-7-6001-2013, 2013.

Guilhermet, J., Preunkert, S., Voisin, D., Baduel, C., and Legrand, M.: Major 20th century changes of water-soluble humic-like substances (HULIS WS) aerosol over Europe inferred from Alpine ice cores, J. Geophys. Res.-Atmos., 118, 3869–3878, doi:10.1002/jgrd.50201, 2013.

Gysel, M., Laborde, M., Olfert, J. S., Subramanian, R., and Gröhn, A. J.: Effective density of Aquadag and fullerene soot black carbon reference materials used for SP2 calibration, Atmos. Meas. Tech., 4, 2851–2858, doi:10.5194/amt-4-2851-2011, 2011.

Hagler, G. S. W., Bergin, M. H., Smith, E. A., Dibb, J. E., Anderson, C., and Steig, E. J.: Particulate and water-soluble carbon measured in recent snow at Summit, Greenland, Geophys. Res. Lett., 34, L16505, doi:10.1029/2007GL030110, 2007.

Hansen, J. and Nazarenko, L.: Soot climate forcing via snow and ice albedos, P. Natl. Acad. Sci. USA, 101, 423–428, doi:10.1073/pnas.2237157100, 2004.

Jacobson, M. Z., Turco, R. P., Jensen, E. J., and Toon, O. B.: Modeling coagulation among particles of different composition and size, Atmos. Environ., 28, 1327–1338, 1994.

Jenk, T. M., Szidat, S., Schwikowski, M., Gäggeler, H. W., Brütsch, S., Wacker, L., Synal, H.-A., and Saurer, M.: Radiocarbon analysis in an Alpine ice core: record of anthropogenic and biogenic contributions to carbonaceous aerosols in the past (1650–1940), Atmos. Chem. Phys., 6, 5381–5390, doi:10.5194/acp-6-5381-2006, 2006.

Jeong, C.-H., Hopke, P. K., Kim, E., and Lee, D.-W.: The comparison between thermal-optical transmittance elemental carbon and Aethalometer black carbon measured at multiple monitoring sites, Atmos. Environ., 38, 5193–5204, 2004.

Kaspari, S. D., Schwikowski, M., Gysel, M., Flanner, M. G., Kang, S., Hou, S., and Mayewski, P. A.: Recent increase in black carbon concentrations from a Mt. Everest ice core spanning 1860–2000 AD, Geophys. Res. Lett., 38, L04703, doi:10.1029/2010gl046096, 2011.

Kondo, Y., Sahu, L., Moteki, N., Khan, F., Takegawa, N., Liu, X., Koike, M., and Miyakawa, T.: Consistency and Traceability of Black Carbon Measurements Made by Laser-Induced Incandescence, Thermal-Optical Transmittance, and Filter-Based Photo-Absorption Techniques, Aerosol Sci. Tech., 45, 295–312, doi:10.1080/02786826.2010.533215, 2011.

Laborde, M., Schnaiter, M., Linke, C., Saathoff, H., Naumann, K.-H., Möhler, O., Berlenz, S., Wagner, U., Taylor, J. W., Liu, D., Flynn, M., Allan, J. D., Coe, H., Heimerl, K., Dahlkötter, F., Weinzierl, B., Wollny, A. G., Zanatta, M., Cozic, J., Laj, P., Hitzenberger, R., Schwarz, J. P., and Gysel, M.: Single Particle Soot Photometer intercomparison at the AIDA chamber, Atmos. Meas. Tech., 5, 3077–3097, doi:10.5194/amt-5-3077-2012, 2012.

Lack, D. A., Moosmüller, H., McMeeking, G. R., Chakrabarty, R. K., and Baumgardner, D.: Characterizing elemental, equivalent black, and refractory black carbon aerosol particles: a review of techniques, their limitations and uncertainties, Anal. Bioanal. Chem., 406, 99–122, doi:10.1007/s00216-013-7402-3, 2014.

Lavanchy, V. M. H., Gäggeler, H. W., Schotterer, U., Schwikowski, M., and Baltensperger, U.: Historical record of carbonaceous particle concentrations from a European high-alpine glacier (Colle Gnifetti, Switzerland), J. Geophys. Res.-Atmos., 104, 21227–21236, doi:10.1029/1999jd900408, 1999.

Legrand, M., Preunkert, S., Schock, M., Cerqueira, M., Kasper-Giebl, A., Afonso, J., Pio, C., Gelencsér, A., and Dombrowski-Etchevers, I.: Major 20th century changes of carbonaceous aerosol components (EC, WinOC, DOC, HULIS, carboxylic acids, and cellulose) derived from Alpine ice cores, J. Geophys. Res., 112, D23S11, doi:10.1029/2006jd008080, 2007.

McConnell, J. R., Edwards, R., Kok, G. L., Flanner, M. G., Zender, C. S., Saltzman, E. S., Banta, J. R., Pasteris, D. R., Carter, M. M., and Kahl, J. D. W.: 20th-century industrial black carbon emissions altered arctic climate forcing, Science, 317, 1381–1384, doi:10.1126/science.1144856, 2007.

Ming, J., Cachier, H., Xiao, C., Qin, D., Kang, S., Hou, S., and Xu, J.: Black carbon record based on a shallow Himalayan ice core and its climatic implications, Atmos. Chem. Phys., 8, 1343–1352, doi:10.5194/acp-8-1343-2008, 2008.

Ming, J., Xiao, C., Cachier, H., Qin, D., Qin, X., Li, Z., and Pu, J.: Black Carbon (BC) in the snow of glaciers in west China and its potential effects on albedos, Atmos. Res., 92, 114–123, doi:10.1016/j.atmosres.2008.09.007, 2009.

Miyazaki, Y., Kondo, Y., Han, S., Koike, M., Kodama, D., Komazaki, Y., Tanimoto, H., and Matsueda, H.: Chemical characteristics of water-soluble organic carbon in the Asian outflow, J. Geophys. Res., 112, D22S30, doi:10.1029/2007JD009116, 2007.

Moteki, N. and Kondo, Y.: Dependence of laser-induced incandescence on physical properties of black carbon aerosols: measurements and theoretical interpretation, Aerosol Sci. Tech., 44, 663–675, doi:10.1080/02786826.2010.484450, 2010.

Ohata, S., Moteki, N., and Kondo, Y.: Evaluation of a Method for Measurement of the Concentration and Size Distribution of Black Carbon Particles Suspended in Rainwater, Aerosol Sci. Tech., 45, 1326–1336, doi:10.1080/02786826.2011.593590, 2011.

Painter, T. H., Flanner, M. G., Kaser, G., Marzeion, B., VanCuren, R. A., and Abdalati, W.: End of the Little Ice Age in the Alps forced by industrial black carbon, P. Natl. Acad. Sci. USA, 1–6, doi:10.1073/pnas.1302570110, 2013.

Petzold, A., Ogren, J. A., Fiebig, M., Laj, P., Li, S.-M., Baltensperger, U., Holzer-Popp, T., Kinne, S., Pappalardo, G., Sugimoto, N., Wehrli, C., Wiedensohler, A., and Zhang, X.-Y.: Recommendations for reporting "black carbon" measurements, Atmos. Chem. Phys., 13, 8365–8379, doi:10.5194/acp-13-8365-2013, 2013.

Preunkert, S., Wagenbach, D., Legrand, M., and Vincent, C.: Col du Dôme (Mt Blanc Massif, French Alps) suitability for ice-core studies in relation with past atmospheric chemistry over Europe, Tellus B, 52, 993–1012, doi:10.1034/j.1600-0889.2000.d01-8.x, 2000.

Preunkert, S., Legrand, M., and Wagenbach, D.: Sulfate trends in a Col du Dôme (French Alps) ice core: a record of anthropogenic sulfate levels in the European midtroposphere over the twentieth century, J. Geophys. Res., 106, 31991–32004, doi:10.1029/2001jd000792, 2001.

Ramanathan, V. and Xu, Y. Y.: The Copenhagen Accord for limiting global warming: criteria, constraints, and available avenues, P. Natl. Acad. Sci. USA, 107, 8055–8062, doi:10.1073/pnas.1002293107, 2010.

Savarino, J. and Legrand, M.: High northern latitude forest fires and vegetation emissions over the last millennium inferred from the chemistry of a central Greenland ice core, J. Geophys. Res. Atmos., 103, 8267–8279, doi:10.1029/97jd03748, 1998.

Schmid, H., Laskus, L., Jürgen Abraham, H., Baltensperger, U., Lavanchy, V., Bizjak, M., Burba, P., Cachier, H., Crow, D., Chow, J., Gnauk, T., Even, A., ten Brink, H. M., Giesen, K.-P., Hitzenberger, R., Hueglin, C., Maenhaut, W., Pio, C., Carvalho, A., Putaud, J.-P., Toom-Sauntry, D., and Puxbaum, H.: Results of the “carbon conference” – international aerosol carbon round robin test stage I, Atmos. Environ., 35, 2111–2121, doi:10.1016/S1352-2310(00)00493-3, 2001.

Schwarz, J. P., Gao, R. S., Fahey, D. W., Thomson, D. S., Watts, L. A., Wilson, J. C., Reeves, J. M., Darbeheshti, M., Baumgardner, D. G., Kok, G. L., Chung, S. H., Schulz, M., Hendricks, J., Lauer, A., Kärcher, B., Slowik, J. G., Rosenlof, K. H., Thompson, T. L., Langford, A. O., Loewenstein, M., and Aikin, K. C.: Single-particle measurements of midlatitude black carbon and light-scattering aerosols from the boundary layer to the lower stratosphere, J. Geophys. Res. Atmos., 111, 1–15, doi:10.1029/2006jd007076, 2006.

Schwarz, J. P., Doherty, S. J., Li, F., Ruggiero, S. T., Tanner, C. E., Perring, A. E., Gao, R. S., and Fahey, D. W.: Assessing Single Particle Soot Photometer and Integrating Sphere/Integrating Sandwich Spectrophotometer measurement techniques for quantifying black carbon concentration in snow, Atmos. Meas. Tech., 5, 2581–2592, doi:10.5194/amt-5-2581-2012, 2012.

Slowik, J. G., Cross, E. S., Han, J.-H., Davidovits, P., Onasch, T. B., Jayne, J. T., Williams, L. R., Canagaratna, M. R., Worsnop, D. R., Chakrabarty, R. K., Moosmüller, H., Arnott, W. P., Schwarz, J. P., Gao, R.-S., Fahey, D. W., Kok, G. L., and Petzold, A.: An inter-comparison of instruments measuring black carbon content of soot particles, Aerosol Sci. Tech., 41, 295–314, doi:10.1080/02786820701197078, 2007.

Stephens, M., Turner, N., and Sandberg, J.: Particle identification by laser-induced incandescence in a solid-state laser cavity., Appl. Optics, 42, 3726–36, 2003.

Ten Brink, H., Maenhaut, W., Hitzenberger, R., Gnauk, T., Spindler, G., Even, A., Chi, X., Bauer, H., Puxbaum, H., Putaud, J.-P., Tursic, J., and Berner, A.: INTERCOMP2000: the comparability of methods in use in Europe for measuring the carbon content of aerosol, Atmos. Environ., 38, 6507–6519, 2004.

Thevenon, F., Anselmetti, F. S., Bernasconi, S. M., and Schwikowski, M.: Mineral dust and elemental black carbon records from an Alpine ice core (Colle Gnifetti glacier) over the last millennium, J. Geophys. Res., 114, D17102, doi:10.1029/2008jd011490, 2009.

Viana, M., Maenhaut, W., ten Brink, H. M., Chi, X., Weijers, E., Querol, X., Alastuey, A., Mikuška, P., and Večeřa, Z.: Comparative analysis of organic and elemental carbon concentrations in carbonaceous aerosols in three European cities, Atmos. Environ., 41, 5972–5983, 2007.

Wang, M., Xu, B., Zhao, H., Cao, J., Joswiak, D., Wu, G., and Lin, S.: The Influence of Dust on Quantitative Measurements of Black Carbon in Ice and Snow when Using a Thermal Optical Method, Aerosol Sci. Tech., 46, 60–69, doi:10.1080/02786826.2011.605815, 2012.

Warren, S. G.: Impurities in snow – effects on albedo and snowmelt review, Ann. Glaciol., 5, 177–179, 1984.

Xu, B., Cao, J., Hansen, J., Yao, T., Joswia, D. R., Wang, N., Wu, G., Wang, M., Zhao, H., Yang, W., Liu, X., and He, J.: Black soot and the survival of Tibetan glaciers, P. Natl. Acad. Sci. USA, doi:10.1073/pnas.0910444106, 2009.

Yang, L., Xiaoye, Z., Sunling, G., Huizheng, C., Dan, W., Wenjun, Q., and Junying, S.: Comparison of EC and BC and evaluation of dust aerosol contribution to light absorption in Xi'an, China, Environ. Monit. Assess., 120, 301–12, doi:10.1007/s10661-005-9062-z, 2006.

Yu, J. Z., Yang, H., Zhang, H., and Lau, A. K. H.: Size distributions of water-soluble organic carbon in ambient aerosols and its size-resolved thermal characteristics, Atmos. Environ., 38, 1061–1071, 2004.

Zanatta, M.: Development of a methodology for deriving black carbon in snow samples: application to Himalayan samples, University of Pavia, Master thesis, 2012.

Table 1. rBC concentrations in snow samples from Col du Dôme (French Alps) determined after different treatment: (a) melting procedure, (b) freezing/melting cycle, (c) surface to volume ratios of the container, and (d) storage. rBC refers to the mean rBC (±1 standard deviation) concentration calculated over *N* samples. Δ(rBC) refers to % variations in rBC concentrations between the reference and the treatment concerned. US stands for ultrasonication. (*) indicates data collected after refreezing and re-melting samples.

N	rBC ($\mu g\ L^{-1}$)	ΔrBC (%)	Treatment description	Re-freezing	rBC ($\mu g\ L^{-1}$)*	ΔrBC (%)*	Treatment description*	Comments
a. Melting procedure								
41	3.4 ± 0.7	*Reference*	Melting at room temp.	X				
	3.4 ± 0.8	0 ± 24	and US 15 min.					
10	3.5 ± 0.3	3 ± 9	30 °C melting	X				
	3.8 ± 0.6	12 ± 18	and US 15 min.					
b. Freezing/melting cycle								
5	4.2 ± 0.9	*Reference*	Melting at room temp.	⇒	2.5 ± 0.9	−40 ± 21	Re-melting at room temp.	
					2.6 ± 0.7	−38 ± 16	and US 15 min.	
5	3.6 ± 0.9	*Reference*	Melting at room temp.	⇒	1.7 ± 0.2	−52 ± 6	Re-melting at room temp.	
					3.1 ± 0.5	−14 ± 14	and US 30 min.	
5	2.8 ± 0.3	*Reference*	Melting at room temp.	⇒	1.5 ± 0.2	−46 ± 7	Re-melting at room temp.	
					2.2 ± 0.7	−21 ± 25	and US 45 min.	
5	2.9 ± 0.3	*Reference*	Melting at room temp.	⇒	1.7 ± 0.3	−41 ± 10	Re-melting at room temp.	
					1.7 ± 0.2	−41 ± 7	and acidification	
c. Surface to volume ratio of the container								
5	3.5 ± 0.6	*Reference*	Melting at room temp.	⇒	2.2 ± 0.5	−37 ± 14	Re-melting at room temp.	
					3.1 ± 0.9	−11 ± 26	and US 30 min.	50 mL PP container
5	5.6 ± 0.9	*Reference*	Melting at room temp.	⇒	2.5 ± 1.7	−55 ± 30	Re-melting at room temp.	125 mL PP container
					3.3 ± 1.9	−41 ± 34	and US 30 min.	
d. Storage								
5	3.5 ± 0.2	*Reference*	Melting at room temp.	X				
	3.6 ± 0.3	3 ± 9	and storage at room temp. for 2 h					
	3.8 ± 0.7	9 ± 20	and storage at room temp. for 4 h					
	3.4 ± 0.4	−3 ± 11	and storage at room temp. for 6 h					
	3.2 ± 0.6	−9 ± 17	and storage at room temp. for 24 h					
5	3.4 ± 0.2	*Reference*	Melting at room temp.	X				
	3.3 ± 0.2	−3 ± 6	and stroage in the regrigerator for 2 h					
	3.2 ± 0.1	−6 ± 3	and stroage in the regrigerator for 4 h					
	3.2 ± 0.1	−6 ± 3	and stroage in the regrigerator for 6 h					
	3.3 ± 0.2	−3 ± 6	and stroage in the regrigerator for 24 h					

Table 2. Summary of inter-comparison of SP2 and thermal-optical methods. All values are ranges and mean ±1 standard deviation in parentheses.

Sample ID	Location	Sample type (*N*)	Sample dating	Filtrated sample volume for EC (mL)	rBC ($\mu g\,L^{-1}$)	EC ($\mu g\,L^{-1}$)	EC/rBC	Filtration efficiency for EC (%)	Dust (ppb)	Total OC loading on filter (µg)	OC ($\mu g\,L^{-1}$)	Pyrolized _OC/ total_OC
SUM	Summit (Central Greenland)	firn (3)	1922–1918 1894–1893 1800–1799	0.9–2.0	1.5–3.0 (2.0 ± 0.9)	1.8–4.6 (3.1 ± 1.4)	0.5–2.9 (1.8 ± 1.2)	50–60	170–393 (262 ± 117)	64.8–229.4 (142.6 ± 82.6)	65.8–153.7 (109.6 ± 44.0)	0.4–0.5 (0.4 ± 0.1)
CDD	Col du Dôme (French Alps, 4250 m a.s.l.)	snow pit (4)	2012–2011	0.2–0.5	7.6–44.9 (16.9 ± 18.7)	0.9–10.9 (4.3 ± 4.5)	0.2–0.7 (0.4 ± 0.2)	30–40	104–10 900 (3059 ± 5246)	6.3–25.4 (11.6 ± 9.3)	15.1–175.6 (81.3 ± 82.9)	0.1–0.6 (0.3 ± 0.2)
ELB	Mt. Elbrus (Caucasus, 5115 m a.s.l.)	firn (5)	2007–2006	0.1–0.2	6.9–26.3 (13.8 ± 8.6)	6.4–33.9 (13.4 ± 11.6)	0.6–1.3 (0.9 ± 0.3)	40	351–1824 (1093 ± 648)	44.3–109.7 (67.8 ± 25.0)	260.6–406.2 (369.8 ± 61.6)	0.4–0.5 (0.5 ± 0.1)
HIM	Himalaya (5079, 5600, 5644 m a.s.l.)	surface snow (8)	2012–2010	0.1–0.2	2.1–22.7 (8.3 ± 7.4)	5.4–57.6 (24.3 ± 20.1)	1.9–5.3 (3.0 ± 1.2)	70–90	232–2339 (1318 ± 842)	21.0–52.2 (38.4 ± 10.3)	105.2–567.9 (359.0 ± 185.2)	0.2–0.6 (0.4 ± 0.1)

Title Page
Abstract | Introduction
Conclusions | References
Tables | Figures
◀| |▶
◀ ▶
Back | Close
Full Screen / Esc
Printer-friendly Version
Interactive Discussion

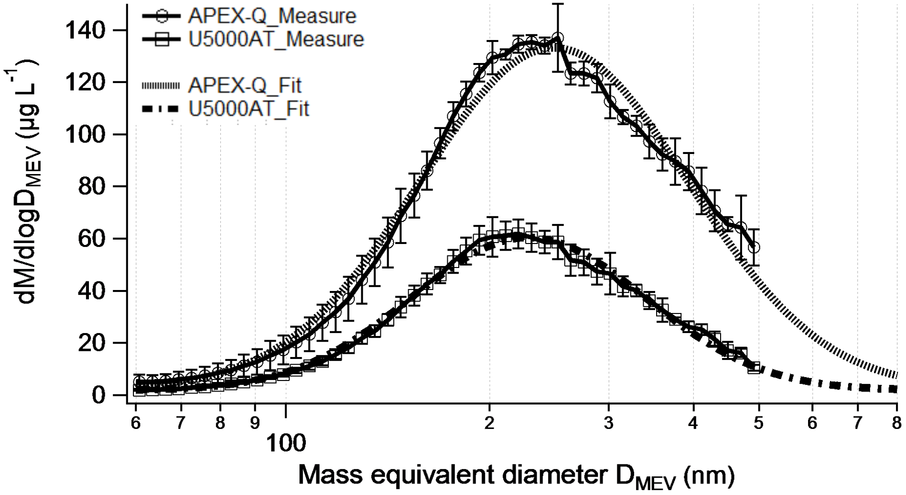

Fig. 1. Mass size distributions of a 100 µg L^{-1} solution of aquadag®, as a function of mass equivalent diameter for APEX-Q and U5000AT nebulizers. The whiskers stand for one standard deviation. Histogram bin size is 50 and log normal fit is between 60 nm and 500 nm.

Title Page
Abstract
Introduction
Conclusions
References
Tables
Figures
◀I
▶I
◀
▶
Back
Close
Full Screen / Esc
Printer-friendly Version
Interactive Discussion

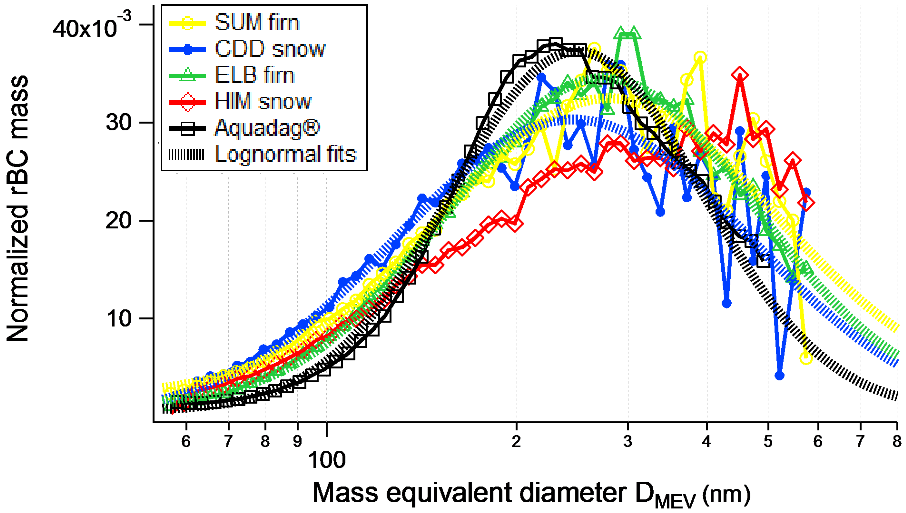

Fig. 2. Mass size distributions of rBC in snow and firn samples from the different sites investigated. The y axis is $\mathrm{d}M/\mathrm{dlog}(D)$ with all distributions normalized to an area of 1. Histogram bin size is 50 and log normal fit is between 60 nm and 500 nm.

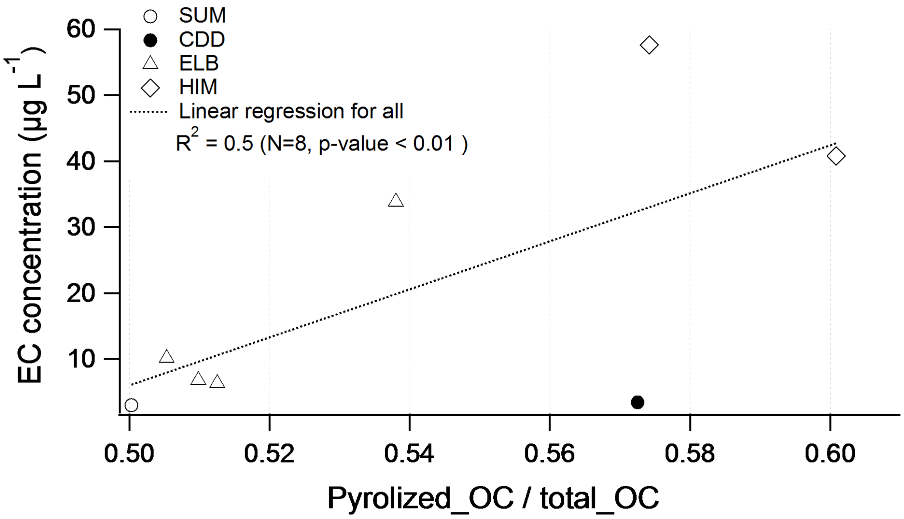

Fig. 3. Comparison of pyrolized_OC/total_OC ratio and EC concentration for all snow and firn samples showing values of pyrolized_OC/total_OC ratio > 0.5.